Silica-Gold Nanoparticles for Atheroprotective Management of Plaques: Results of NANOM-FIM Trial

Silica-Gold Nanoparticles for Atheroprotective Management of Plaques: Results of NANOM-FIM Trial

Alexander N. Kharlamov [1-3*], Anastasiya E. Tyurnina[4], Vera S. Veselova[2, 3], Olga P. Kovtun[3], Vladimir Y. Shur[4], Jan L. Gabinsky[2, 3] on behalf of the team of *NANOM FIM* study

[1]De Haar Research Foundation, Rotterdam, The Netherlands

[2]Department of Science, Department of Interventional Cardiology, Ural Institute of Cardiology, Yekaterinburg, Russia

[3]Division of Science, Ural Medical University, Yekaterinburg, Russia

[4]Ural Center of Modern Nanotechnologies, Institute of Natural Sciences, Ural Federal University, Yekaterinburg, Russia

* Correspondence:

Dr. Alexander Kharlamov,

De Haar Research Foundation

Handelsplein 15

Rotterdam 3071 PR,

The Netherlands

Phone: +31642666912, +79679074063

E-mail: drkharlamov@icloud.com

Short/ running title: Photothermal therapy of atherosclerosis

Abstract word-count: 224
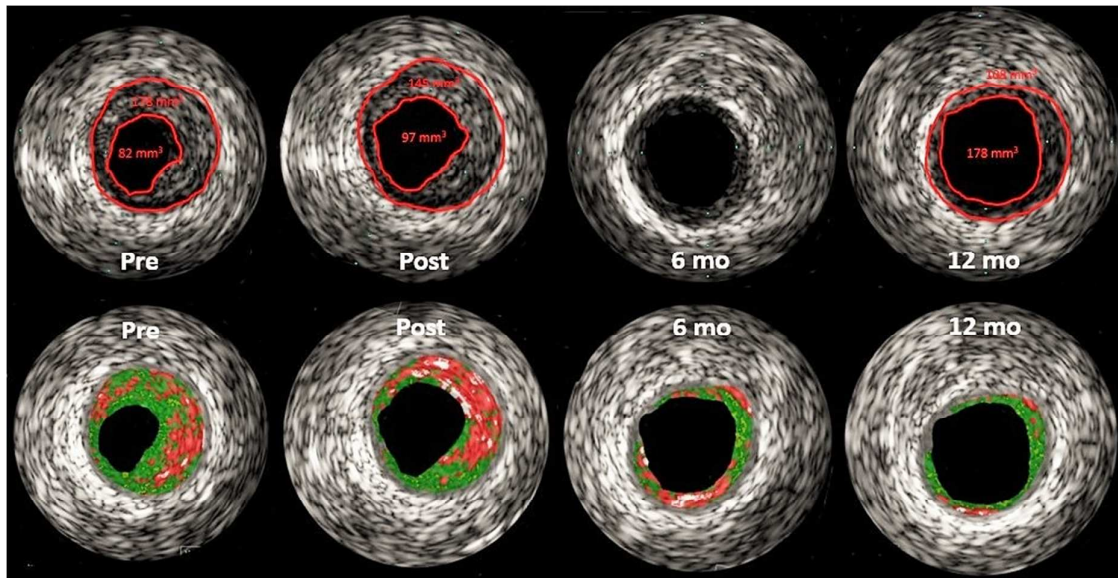
Table of content entry word-count: 49

Word-count: 4495

Number of tables: 4

Number of full-color figures: 1

Number of black-and-white figures: 3

Table of contents entry

Atheroregression below 40% Glagov threshold becomes an attractive target for cardiovascular treatment. Proposed nanotechnology using silica-gold nanoparticles associated with the mean total atheroma volume reduction of 60.3 mm^3 (p<0.05) at 12 months in group underwent photothermal therapy up to 37.8% (p<0.05) plaque burden promising to revolutionize interventional vascular medicine.

ABSTRACT

Background

Atheroregression becomes an attractive target for cardiovascular treatment. Some clinical trials have demonstrated that intensive therapy with rosuvastatin or recombinant ApoA-I Milano can partially reduce the total atheroma volume (TAV) up to 6.38 mm^3 or 14.1 mm^3 respectively. Our previous bench studies of selected nanotechnologies documented TAV reduction up to unprecedented 79.4 mm^3.

Methods

The completed observational three arms (n=180) first-in-man trial (the NANOM FIM trial) assessed (NCT01270139) the safety and feasibility of two delivery techniques for nanoparticles (NP), and plasmonic photothermal therapy (PPTT). Patients were assigned to receive either (1) nano-intervention with delivery of silica-gold NP in bioengineered on-artery patch (n=60), or (2) nano-intervention with delivery of silica-gold iron-bearing NP with targeted micro-bubbles and stem cells using magnetic navigation system (n=60) versus (3) stent implantation (n=60). The primary outcome was TAV at 12 months.

Results

The mean TAV reduction at 12 months in Nano group was 60.3 mm^3 (SD 39.5; min 41.9 mm^3, max 94.2 mm^3; $p<0.05$) up to mean 37.8% (95% CI: 31.1%, 51.7%; $p<0.05$) plaque burden. The analysis of the event free survival of the ongoing clinical follow-up shows the significantly lower risk of cardiovascular death in Nano group when compared with others (91.7% vs 81.7% and 80% respectively; $p<0.05$) with no cases of the target lesion-related complications.

Conslusions

PPTT using silica-gold NP associated with significant regression of coronary atherosclerosis.

Key-words: nanomedicine, silica-gold nanoparticles, plasmonic photothermal therapy, atheroregression, stenting.

INTRODUCTION

The reversal of atherosclerosis below becomes a new attractive target for cardiovascular therapy and coronary device development[1, 2].

Some clinical trials have demonstrated that lowering LDL levels through intensive statin therapy while accompanied by raised HDL, can slow progression, or even partially reduce the total atheroma volume (up to 6.38 mm^3) in coronary arteries[1, 2]. Of note, plaque regression was associated only with a 30% relative reduction in events. By the way of comparison, recombinant ApoA-I Milano demonstrated a 14.1 mm^3 reduction in total atheroma volume[3].

Plasmonic photothermal therapy (PPTT) using near-infrared (NIR) laser irradiation[4-6] is the novel invasive approach in cardiology. The noble-metal nanoparticles are the only type of optically active composite spherical particles on the nanoscale[7-9] for needs of PPTT. Our previous bench studies PLASMONICS[10] documented acceptable level of safety and significant efficacy of PPTT with unprecedented plaque burden (PB) reduction up to 79.4 mm^3.

The first-in-man trial (the NANOM FIM trial) assessed the safety and feasibility of two delivery techniques for NP, and PPTT of atherosclerotic lesions in patients with coronary artery disease (CAD) and SYNTAX score ≤22.

METHODS

Study Population and Procedures

This trial was a multi-center (two sites), observational, open-label, three arms study in 180 patients with CAD and angiographic SYNTAX score ≤22. The protocol was approved by the Ethics Committee and the Research Steering Committee of the Ural State Medical University (Yekaterinburg, Russia). The study is registered in clinicaltrials.gov with identifier NCT01270139. All participants signed written informed consent before enrollment. The project started in April, 2007 and completed in June, 2012. After the technology development in September 2004, a series of animal experiments[10] described as PLASMONICS study were performed in 2004-2007. On the basis of excellent experimental results, the ethics committee of the Ural Institute of Cardiology (Yekaterinburg, Russia) under the supervision of the Medical University permitted the start of human interventions.

Diseased patients, men and women, aged 45-65 years were enrolled if they were judged to have single- or multi-vessel CAD with flow-limiting lesions and without indications for coronary artery bypass surgery (CABG), stable angina with indications for percutaneous coronary interventions (PCI), NYHA (New York Heart Association) I-III functional class of heart failure (HF), treated hypertension (in supine position: systole >140 mm Hg, diastole >90 mm Hg). All patients with history of PCI were allocated if they did not have anamnesis of myocardial infarction (MI). Exclusion criteria included non-compliance, angiographic SYNTAX score ≥23, history of MI, unstable angina, or CABG, atrial fibrillation or other arrhythmias, stroke; indications for CABG, contraindications for PCI or CABG; NYHA IV functional class of HF, diabetes mellitus (in case of fasting glucose >7.0 mM/L or random glucose >11.0 mM/L), untreated hypertension, asthma, known hypersensitivity or contraindications to anti-platelet drugs, contrast sensitivity, and participation to any drug- or intervention-investigation during the previous 60 days.

Target lesions were selected if they had less than 3.0 mm in diameter and 10 mm in length by visual estimation, a stenosis of between 50% and 99% of luminal diameter with a TIMI (Thrombolysis in Myocardial Infarction) flow grade of 1 or more with a total atheroma volume (TAV) of the target lesion at least 100 mm^3 (minimal vessel volume – at least 200 mm^3) as assessed by online quantitative coronary angiography (QCA) or intravascular ultrasound (IVUS). Patients were ineligible if they had any of the following: left main coronary artery stenosis, an ostial lesion, lesion located within 2 mm of a bifurcation; lesion with moderate-to-heavy calcification by visual assessment; angiographically visible thrombus within the target lesion.

Patients who met the inclusion criteria were assigned (the intention-to-treat population, ITTP) in a 1:1:1 ratio to receive (see fig. 1) either (1) nano-intervention with delivery of silica-gold nanoparticles (NP) in mini-surgery implanted bioengineered on-artery patch (n=60), or (2) nano-intervention with delivery of silica-gold iron-bearing NP with targeted micro-bubbles and stem cells using magnetic navigation system (n=60).

In control group, XIENCE V stent (Abbott Vascular, Santa Clara, CA) was implanted to 60 patients. Patients with a single de novo native coronary stenosis were stented by a single stent of 3.0 x 18 mm. The implantation had to be performed according to common interventional practices including the administration of intracoronary nitroglycerine 0.2 mg of glycerol trinitrate or isosorbide dinitrate and intra-arterial heparin

(50-100 U/kg body weight). Pre-dilation with a conventional balloon catheter (with a pressure not exceeding the rated-burst pressure 16 atm) was recommended before drug-eluting stent (DES) deployment according to the manufacturer's recommendation. The protocol recommended the study stent should cover 2 mm of non-diseased tissue on either side of the target lesion. Post-dilation was allowed with a balloon that was shorter than was the study device.

Some patients were excluded from the per-treatment-evaluable population (PTEP) if they had a history of PCI, or received a stent in addition to the study device (if interpreted as target vessel revascularization - TVR), or were treated with CABG (if interpreted as target lesion revascularization - TLR). Patients were also excluded from PTEP in case of non-compliance or documented diabetes, NYHA IV functional class of HF, or SYNTAX score ≥23. The ITTP population was our primary population.

The primary outcome was TAV (plaque-media volume, mm^3) at 12 months. The secondary outcomes were per cent atheroma volume (PAV, plaque burden, %), composition of plaque (per cent of fibro-fatty component, per cent of fibrous component, per cent of necrotic core, per cent of calcium), minimal lumen diameter (MLD, mm), event free survival, TLR, restenosis rate (stenosis >50%), late definite thrombosis rate, and coronary vasomotion at 12 months. Imaging and clinical end-points were assessed pre-, post- procedure and at 12-month follow-up.

We defined a clinical device success as successful delivery of NP or implantation of stent at the target lesion. The procedure of NP delivery was IVUS- and QCA-guided (see fig. 2a). Clinical procedure success was defined as above without the occurrence of major adverse clinical events related to ischemia up to 7 days after the index procedure. All major adverse cardiac events were adjudicated by an independent clinical events committee, and a data safety monitoring board monitored patient safety. Ten per cent of QCA and IVUS data were analyzed by independent CoreLab (Orenburg, Russia). The SYNTAX (SYNergy between percutaneous coronary intervention with TAXus and cardiac surgery) score was calculated using the calculator which is available online (www.syntaxscore.com). All variables pertinent to calculation were computed by three interventional cardiologists who were blinded to procedural data and clinical outcome.

Nanotechnologies and methods of PPTT

The 60/15-70/40 nm core/ shell silica-gold NP were fabricated with a modified aqueous-phase method as described previsouly[10, 27]. Fe_3O_4 magnetic silica-gold NP with diameters of approximately 90-150 nm were prepared according to solvothermal and co-precipitation methods as described in the previous studies[10, 24]. The NP were characterized with transmission electron microscopy (TEM). NP exhibit a broader plasmonic resonance at 815-821 nm. Modified CD68 targeted gas(perfluoropropane)-filled protein(albumin)-coated micro-bubbles were constructed as previously described[10, 19]. Allogenious and purified cells with initial CD45^{-}, CD34^{-}, CD73^{+} and CD105^{+} markers were used for the growing of the bioengineered on-artery patch as described in PLASMONIC pre-clinical study[10, 16]. Briefly, a patch composed of the sliced porous bovine pericardium biological scaffold with inserted growing multilayered purified allogeneic stem cells with initial mesenchymal phenotype. NP were cultivated in the medium with stem cells and micro-bubbles in order to achive the maximum concentration of uploaded NP in the cell or albumin micro-bubble. In the prepared medium with stem cells (mean size - 24±20 μm) and solution with micro-bubbles (mean size - 4±3 μm), the

concentration of silica-gold NP was approximately 43 nM (2.23 mg/mL) and 39 nM (1.64 mg/mL) respectively, while the concentration of silica-gold iron-bearing NP was approximately 45 nM (2.12 mg/mL) and 41 nM (1.93 mg/mL) respectively. In each stem cell, there were 158±134 silica-gold NP, and 122±104 silica-gold iron-bearing NP. NP were detonated by percutaneous transcatheter intravascular or out-of-body transcutaneous intercostal NIR laser irradiation (microwatt NIR laser, 821 nm, 35-44 W/cm^2 for 7 min of exposure). The characteristics of NIR laser were adjusted individually by the body-mass index, thickness of skin and hypodermic tissue, or vessel and plaque dimensions in order to optimize the mean dose of irradiation and plasmonic effect in the personalized fashion.

Patients in Nano group (fig. 1) were treated with bioengineered patch that was grown with allogenious stem cells pre-cultivated in the medium with NP. After the admission, patients were examined with QCA, and allocated to the trial. The implantation of the patch onto the artery was undergone by the minimally invasive cardiac surgery (MICS CABG) with fixation of the graft to the epicardial myocardium. So called MICS CABG or the McGinn technique implies a beating-heart multi-vessel heart surgery performed through several small (stretch no more than up to 5-7 cm) incisions under direct vision through an aterolateral mini-thoracotomy in the 4th-6th intercostal spaces. The approach is considered as an alternative to PCI allowing quick recover without major complications. The patients can expect high quality of life resuming all everyday activities within a few weeks of their operation. NP were activated with NIR laser at 7 days after the intervention under the QCA- and IVUS-guidance at the Acute Care Unit. Patients were treated with bolus of bivalirudin on the day of NP detonation.

Patients in Ferro group (fig. 1) were managed with intracoronary infusion of allogenious stem cells (average 6x10^6) and CD68 targeted micro-bubbles (average 1660.2 per mL) pre-cultivated in the medium with iron-bearing NP. After the admission, patients were examined with QCA, and allocated to the trial. The 1:1 suspension of cells and micro-bubbles were infused to the target coronary artery via micro-catheter on the day of admission at the Acute Care Unit. The destruction of CD68 targeted micro-bubbles was obtained by using a Sonos 5500 machine (Agilent Technologies) with an S3 transducer operating in ultraharmonic mode (transmit, 1.3MHz/ receive, 3.6 MHz) with a mechanical index of 1.5 and a depth of 4 cm. The transducer was placed on the thorax in a mid short-axis view. The burst every four cardiac cycles episodically destroyed the micro-bubbles in the arteries, which was easily monitored by complete reduction of the opacification. The AXIOM Artis dBC (Siemens) magnetic navigation system was used for precise delivery of NP to the atheroma through two permanent computer-controlled external magnets generating a navigational magnetic field of 0.08 Tesla in any direction with opportunity to produce a spot at the site of target vessel and lesion. The size and shape of magnetic spot were tailored by the parameters of heart motion and displacement of coronary artery in the thoracal space. NP were detonated with NIR laser at the end of the procedure under the protection of anti-platelet therapy.

Imaging analysis

Quantitative coronary angiography (QCA) and Intravascular Ultrasound (IVUS) were performed pre-, post-procedure and at 12-month follow-up after a bolus infusion of i.c. nitrate. The imaging was undergone with analysis of different parameters such as minimal lumen diameter, maximum lumen diameter, reference

diameter, diameter stenosis, lesion length, percent atheroma volume (PAV), total atheroma volume (TAV), and lumen volume. The PAV was calculated as follows:

$$PAV = \frac{\Sigma\,(EEM_{area} - lumen_{area})}{\Sigma\,EEM_{area}} \times 100$$

where EEM_{area} is the cross-sectional area of the external elastic membrane, and $lumen_{area}$ is the cross-sectional area of the lumen. The change in PAV was calculated as the PAV at 12 months minus the PAV at baseline. The TAV was calculated as follows:

$$TAV_{normalized} = \frac{\Sigma\,(EEM_{area} - lumen_{area})}{\text{no. of images in pullback}} \times \frac{\text{median no. of}}{\text{images in cohort}}$$

The efficacy end-point of change in normalized TAV was calculated as the TAV at 12 months minus the TAV at baseline. Regression was defined as a decrease in PAV or TAV from baseline.

This evaluation was carried out centrally by the independent angiographic CoreLab of the Heart Clinic (Yekaterinburg, Russia) by two independent operators. A difference of ±3% of the relative parameter (%) between the two readings was accepted. If the discrepancy exceeded this value, the third operator decided upon the result of the assessment. IVUS and IVUS-VH (virtual histology) images were acquired simultaneously with a phased array 40 MHz intravascular ultrasound catheter (Volcano Co., Rancho Cordova, CA; or Boston Scientific Scimed, Inc, Maple Grove, MN) with motorized pull-back at a constant speed of 0.5 mm/s (fig. 2a) over a length of 10 mm to 80 mm. Four tissue components (necrotic core – red; dense calcium – white; fibrous – green; and fibro-fatty – light green or yellow) were identified with autoregressive classification systems. For each cross section stent struts were detected as areas of apparent dense calcium and necrotic core. All IVUS analysis was performed offline by a CoreLab of the Heart Clinic.

Coronary vasomotion was assessed with QCA. End-diastolic images of coronary arteries were evaluated at baseline, after intravascular infusion of acetylcholine (Ach) (through a microcatheter at increasing doses up to 10^{-8}, 10^{-7}, 10^{-6} M with a washout period of at least five minutes between each dose), and after nitroglycerine application following Ach (100 µg orally). In all patients, measurements were performed in two segments on site of intervention while 960 seconds. The artery diameter was calibrated against the contrast-filled tip of the catheter. Vasoconstriction to Ach was defined as a 3% change of the mean lumen diameter after infusion of the maximal dose of Ach. An investigator blinded to treatment group performed all measurements.

Definitions

Myocardial infarction was defined in accordance with the joint ESC/ACCF/AHA/WHF universal definition of myocardial infarction (Thygesen K, et al. Eur Heart J 2007), and then re-validated by the guidelines of the European Society of Cardiology for the third universal definition of myocardial infarction (Thygesen K, et al. Eur Heart J 2012).

Non-compliance was defined as a broad concept and included noncompliance with the protocol, standard operating procedures, GCP and/ or applicable regulatory requirements by an investigator/ institution, or by members of the sponsor's staff in accordance with Good Clinical Practice guidelines. All the cases of non-compliance were assessed by the independent Research Steering Committee.

Concomitant medication

Aspirin was administered $\geq$ 100 mg daily orally for $\geq$ two days pre-intervention. A loading dose of 300 mg of clopidogrel was applied at least six hours before procedure. Bivalirudin 1 mg/kg bolus was provided for patients at the day of intervention. Aspirin 50-100 mg orally daily with clopidogrel 75 mg orally daily were scheduled for six months. All the patients were treated with statin drugs (atorvastatin 40 mg or rosuvastatin 40 mg by the Russian Public Health program) for years prior to the study. Rosuvastatin 40 mg orally daily was prescribed for life to all patients. Hypertension and heart failure were treated with beta-blockers, angiotensin II receptor antagonists, diuretics, and long-acting calcium channel blockers.

Statistics

The Kolmogorov-Smirnov test was used to prove Gaussian distribution allowing for calculation of the mean and standard deviation. Non-Gaussian samples are described by median and range. Discriminant variables are evaluated with the two-sided Fisher's exact test. Continuous variables are compared with student's unpaired t-test. Differences between three groups were analyzed by means of a repeated-measures 1-way ANOVA followed by a Fisher's post hoc test. IVUS efficacy end points are reported as medians, with distribution-free 95% confidence intervals, and intervention groups were compared with the use of analysis of covariance on rank-transformed data after adjustment for baseline values. For all tests the significance level α is 0.05. Statistical analysis was performed with SPSS 20.0 software (SPSS Inc., Chicago, IL).

RESULTS

Table 1 shows baseline characteristics of the population. The procedure was a success in all 180 patients, and device success (calculated on a per-device basis) was 100%. The minimum duration of follow-up was 369±10 days. All the patients were thoroughly tested before intervention in order to reduce a risk of the procedure-related complications and optimize results. Up to 12 months we recorded no instances of life-threaten complications or thrombosis at the site of intervention.

Table 2 demonstrates results of the imaging (QCA and IVUS) analysis post-procedure and at 12-month follow-up. The reduction of the PAV (PB) post-procedure/ at 12-month follow-up was 12.6%/44.8%, 13.1%/43.2%, 20.2%/22.7% (p<0.05 for comparisons between two nano-groups and control) in Nano, Ferro and Control groups of the ITTP respectively (fig. 2, b-e). The mean TAV reduction in Nano group was 60.3 mm^3 (SD 39.5; min 41.9 mm^3, max 94.2 mm^3).

The increase in MLD (fig. 2f) from baseline to post-procedure/ at 12-month follow-up was 5.9/ 63.6%, 21.2/ 63.8%, 56.2/ 62.4% in groups respectively. Despite the 'bumpy' and dilative changes (fig. 2b) in the lumen dimensions, we have documented only one case of the definite thrombosis (table 3) at the site of intervention in Ferro group with three events of the TLR in both Nano and Ferro groups. IVUS analysis also has shown (fig. 2b) the late lumen enlargement with signs of proper endothelial recovery and progressive restoration of the injured artery wall.

The serial assessments of VH-IVUS (fig. 3) showed a significant decrease at 12 months in the dense calcium area, fibrous and fibro-fatty tissue in nano groups, whereas we measured an increase of fibrous and fibro-fatty components in stenting control group. Our observations document significant increase in necrotic core post-procedure with further reduction in size at 12-month follow-up.

There was statistical heterogeneity of hazard ratio between subgroups (table 4) for the primary end point, with greater regression of PAV in Nano group as compared with Ferro or control groups in patients with smaller baseline size of necrotic core (p=0.03) and larger baseline fibro-fatty component (p=0.04).

For 120 patients in both studied groups at 12 months we recorded binary stenosis in four patients (3.3%) - two cases per group. The Kaplan-Meier analysis of the event free survival (table 3) of the ongoing clinical follow-up shows the significantly lower risk of cardiovascular death in Nano group if compare with others (91.7% vs 81.7% and 80% respectively; p<0.05). Those five cases of death as well as three cases of myocardial infarction in Nano group were not associated with target lesion. One patient was stented with XIENCE V stent at the target lesion due to restenosis at 11 months after the intervention.

All patients were undergone vasomotion tests. Overall, the increase in the mean lumen diameter after Ach administration (fig. 4a) was 2.89% (p=0.053), 3.84% (p=0.058), and 1.04% (p=0.12) in groups respectively. 178 patients (98.9%) exhibited a slight vasodilatory response to Ach, whereas 2 patients (1.1%) had an abnormal response to Ach with vasoconstriction. The analysis of cumulative frequency for the changes in mean lumen diameter (fig. 4b) shows significantly (p<0.0001) higher vasodilatory sensitivity of arteries to Ach in nano groups if compare with stenting control.

We did not document any changes in the level of cholesterol at 12 months with concomitant treatment by rosuvastatin 40 mg orally daily. The level of LDL (low-density lipoprotein) cholesterol has been changed

from 1.64 (95% CI: 1.61-1.78) to 1.78 (95% CI: 1.66-1.80) mmol per liter at 12 month after the nano-intervention or stenting (p>0.05). The HDL (high-density lipoprotein) cholesterol decreased from 1.32 (95% CI: 1.30-1.34) to 1.29 (95% CI: 1.27-1.33) mmol per liter (p>0.05 for all comparisons) in groups.

DISCUSSION

Current PCI using DES generally just manipulates the form of the plaque and has some clinical and technical limitations as well as relatively high complication rate[1]. As in the porcine model with bioresorbable scaffolds (BRS) implantation, late lumen enlargement, and plaque-media reduction (12.7%) with wall thinning were observed in humans using IVUS[2, 10, 12, 13]. By comparison, in the most recent study of plaque regression in patients receiving rosuvastatin, the relative reduction in plaque-media volume was 8.5% over a period of 2 years[1, 2]. Numerous devices utilizing heat and high-energy light such as laser technology (excimer ultra-violet laser)[14], electrosurgical approach, radio frequency sparking have been also described as the applications to treat atheroma[15-23]. Plasmonics offers a novel solution for atherodestruction heralding a new era of the manageable atheroregression in cardiology[24-33] with possibility to reverse atherosclerosis.

Our previous bench studies[10] in Yucatan mini-swines have established feasibility and significant benefit of PPTT for atheroregression with mean reduction of PB up to 79.4 mm^3, acceptable level of safety, and no evidences of cytotoxicity. Among five available techniques for delivery of NP we have selected three approaches with maximal safety that use (1) transcatheter intravascular infusion or injection to the lesion of the pre-incubated with NP autologous stem cells, (2) mini-invasive cardiac surgery transplantation of bioengineered on-artery patch (to the projection of culprit lesion) grown with stem cells bearing NP, and (3) transcatheter intravascular infusion or injection of the iron-bearing NP with stem cells or targeted protein-coated microbubbles, and delivery using magnetic fields. Last two techniques demonstrated the relatively high accumulation of NP in the target lesion and low risk of acute plaque rupture or acute thrombosis at the site of intervention that was warranted and deemed appropriate for further tests in humans.

This study compared two different approaches for delivery of NP with the main goal to destruct the target atheroma with acceptable for the real clinical practice level of safety and efficacy. The regression of PB was achieved in both experimental groups with high level of safety, unprecedented reduction of TAV up to 60 mm^3 (more than 92% of patients in Nano group), and late lumen enlargement without signs of positive or negative artery remodeling.

Recently cardiology is searching for an optimal target in treatment of atherosclerosis – from the routine restoration of the lumen dimensions and delaying of atherogenesis to atheroregression and reparative vascular therapy. Currently, the maximum success of conventional therapy with drugs was documented on the level of 6 mm^3 with rosuvastatin[1], and a 14 mm^3 - in studies of ApoA-I Milano[3]. Definitely, this is about incomparable populations of patients, but these two examples demonstrate very well a certain threshold for current therapeutic approaches. Moreover, pledging data from the group of Prof. Emelianov[31] demonstrated that IVUS with photoacoustic imaging provides a platform for detection and temperature monitoring of atherosclerotic plaques through the selective heating of plasmonic gold nanoparticle contrast agents overwhelmingly confirming feasibility of PPTT, which gives a chance to conquer the atherosclerosis, dramatically decreasing TAV, reducing cardiovascular mortality and improving quality of life. In fact, our study registered no target lesion major adverse cardiac events (MACE). The precise nature of the relationship between prevention of MACE and PB reduction remains a subject of ongoing research. Theoretically, regression involves reductions of the lipid, inflammatory, and necrotic components of plaque, each of which

has been implicated in plaque rupture. And indeed our study documented reduction of the necrotic core, fibrous and fibro-fatty components as well as dense calcium by results of VH-IVUS analysis at 12-month follow-up.

The explanation of the working mechanism for PPTT is a major challenge in the current studies. The influence of the following tissue-destructive factors of PPTT, which was called 'cooking' with NIR laser[6, 7, 9, 26], is expected: high-heat plasmonic detonation of nanoshells with thermo-mechanical damage (including 'fulminant' necrosis) of targeted tissues, vapor bubbling of cellular cytoplasm and extracellular matrix with subsequent degradation and melting of tissues, and destructive effects of acoustic and shock waves with supersonic expansion. There are two main physical mechanisms that could lead to the laser-induced explosion of nanoparticles - thermal explosion mode through electron-photon excitation-relaxation, and Coulomb explosion mode through multiphoton ionization[28, 29]. Thermal explosion mode of PPTT implies a thermal explosion of nanoparticles which occurs when heat is generated within the strongly-absorbing target more rapidly than the heat can diffuse away[30]. VH-IVUS analysis in our study demonstrated significant enhancement of the necrotic core immediately after the NP detonation that correlates with above-described plasma-thermolytic mechanism of the PPTT. The clinical value of PPTT in case of the vulnerable plaque with large necrotic core and thin cap is another target for the running clinical trials.

The potential for restoration of vasomotion at 12 months with predominantly vasodilatory response to Ach hypothetically underlines the recovery of the vessel wall architecture after PPTT with proper re-endothelialization and physiological function of smooth muscle cells. The mechanism of the tissue repair after the intervention requires further bench investigations. Injured or 'burned' areas probably were restored by 'inflammatory' and stem or progenitor cells from the resident tissues, niches in adventitia and circulation. A role of transplanted allogenious stem cells as both carriers of NP and bioactive substances for the local regulation of tissue repair still requires clarification in the pre-clinical investigations. The reduction of the dense calcium by VH-IVUS data is also an argumentative evidence of the stem cell benefits for the physiological remodeling of the artery after aggressive PPTT.

One of the key limitations of this approach is the optimal technique of the NP delivery into the target tissue of the culprit atheroma. The delivery of NP with bioengineered patch has had more pronounced effect for atheroregression with more significant level of safety. Potentially, both studied approaches of delivery are of great importance for the further clinical development, but still being relatively aggressive and traumatic for patients. The potential progress of the proposed technology includes development of two different approaches for delivery with utilization of stem cells as the main carriers for NP. The first approach is more applicable for patients with indications for PCI and implicates micro-infusion trans-catheter (Cricket or Bullfrog micro-infusion catheters of Mercator Medical Systems, San Leandro, CA) intramural injection of stem cells into the artery or perivascular tissues under the control of the advanced imaging. The second strategy concerns patients with indications for CABG, and includes growing of the bioengineered patch as a carrier for stem cells with the subsequent MICS CABG transplantation.

An absence of the solution to acutely or urgently maintain the lumen remains another technical and clinical limitation for above-mentioned nano-approach. Both the transient implantation of BRS and high-

energy NIR laser angioplasty represent potentially very elegant tools for real clinical practice in case when the urgent restoration of blood flow is required. The combination of NIR angioplasty (maintain of the lumen) with NIR spectroscopy (intravascular imaging) and NIR laser detonation of NP inside the lesion (management of the entire plaque) is able to secure the high clinical theranostic value of NIR technologies.

Limitations

The study was launched as a PROBE (prospective randomized open blinded end-point) trial. Patients were randomly enrolled to three groups, but design was partly broken due to emergent medical reasons, significant difference of the procedures, and impossibility to calculate sample size due to absolute novelty of the technology and absence of the appropriate clinical trials for the calculation of the required number of patients.

End-points were evaluated by a blinded end-point committee. The study was formally continued as under-powerful three-arm observational clinical trial with blind assessment of results. The sample size was not defined on the basis of an end-point hypothesis, therefore the present FIM study should be considered as hypothesis-generating. The third arm with stenting control was created in order to compare nanotechnologies with conventional implantation of the well-studied second generation stent that previously demonstrated superiority or at least non-inferiority to another stents in series of clinical trials.

Perspectives

There is certainly a room for the further research and technology development at this field in order to optimize this approach for real clinical practice and revolutionize interventional cardiology. The beneficial properties of gold nanoparticles carry a challenge to optimize near-infrared (NIR) imaging and use its plasmonic "pleiotropic" effects for both imaging and photothermal treatment of atherosclerosis. NIR technologies offer the potential to be used for NIR spectroscopy, angioplasty (analogous to excimer laser), nano-amplification for any imaging modalities, and activation or detonation of nanoparticles for plasmonic photothermal therapy.

Conclusion

Plasmonic resonance therapy using silica-gold NP associated with significant regression of coronary atherosclerosis. Both approaches for delivery of NP have acceptable for clinical practice level of safety as well as similar degree of regression of TAV in favor of the minimally invasive cardiac surgery implantation of the bioengineered patch onto the artery.

Conflict of interest

References

1.   S. J. Nicholls, C. M. Ballantyne, P. J. Barter, *NEJM*, 2011, **365**, 2078-87.

2.   Y. Onuma, T. Muramatsu, A. Kharlamov, P. W. Serruys, *Cardiovasc. Interv. Ther.*, 2012, **27(3)**, 141-154.

3.   S. Nissen, T. Tsunoda, E. M. Tuzcu, *JAMA*, 2003, **290**, 2292-2300.

4.   J. R. McCarthy, *Curr. Cardiovasc. Imaging Rep.*, 2010, **3**, 42-49.

5.   B. Godin, J. H. Sakamoto, R. E. Serda, A. Grattoni, A. Bouamrani, M. Ferrari, *Trends Pharmacol. Sci.*, 2010, **31(5)**, 199-205.

6.   L. R. Hirsch, *Proc. Natl. Acad. Sci. USA*, 2003, **100**, 13549–13554.

7.   I. L. Maksimova, G. G. Akchurin, B. N. Khlebtsov, *Medical Laser Application*, 2007, **22**, 199-206.

8.   N. Khlebtsov, G. Akchurin, B. Khlebtsov, *SPIE*, 2008, **9**, 1-3.

9.   D. Pissuwan, S. M. Valenzuela, M. B. Cortie, *Trends Biotechnol.*, 2006, **24**, 62–67.

10.   A. Kharlamov, J. Gabinsky, *Rejuvenation Research*, 2012, **15(2)**, 222-230.

11.   S. Glagov, E. Weisenberg, C. K. Zarins, *NEJM*, 1987, **316(22)**, 1371-5.

12.   P. W. Serruys, H. M. Garcia-Garcia, Y. Onuma, *Eur. Heart. J.*, 2012, **33(1)**, 16-25.

13.   J. A. Ormiston, P. W. Serruys, Y. Onuma, R. J. van Geuns, Circulation: *Cardiovasc. Interv.*, 2012, **5(5)**, 620-32.

14.   Y. E. Appelman, J. J. Piek, S. Strikwerda, *Lancet*, 1996, **347(8994)**, 79-84.

15.   M. E. Lobatto, V. Fuster, Z. A. Fayad, W. J. Mulder, *Nature Rev. Drug. Discov.*, 2011, **10(11)**, 835-52.

16.   L. M. Ricles, S. Y. Nam, K. Sokolov, S. Y. Emelianov, *Int. J. Nanomedicine*, 2011, **6**, 407-16.

17.   K. Homan, J. Shah, S. Gomez, *J. Biomed. Opt.*, 2010, **15(2)**, 021316.

18.   J. Tang, M. E. Lobatto, J. C. Read, A. J. Mieszawska, Z. A. Fayad, W. J. Mulder, *Curr. Cardiovasc. Imaging Rep.*, 2012, **5(1)**, 19-25.

19.   D. R. Lewis, K. Kamisoglu, A. W. York, P. V. Moghe, *WIREs Nanomed. Nanobiotechnol.*, 2011, **3**, 400-20.

20.   P. A. Lemos, V. Farooq, C. K. Takimura, P. S. Gutierrez, R. Virmani, F. Kolodgie, U. Christians, M. Doshi, P. Sojitra, A. Kharlamov, H. M. M. van Beusekom, P. W. Serruys, *EuroIntervention*, 2013, **9(1)**, 148-56.

21.   A. Jayagopal, M. F. Linton, S. Fazio, F. R. Haselton, *Curr. Arterioscler. Rep.*, 2010, **12(3),** 209-215.

22. S. S. Yu, R. A. Ortega, B. W. Reagan, J. A. McPherson, H. J. Sung, T. D. Giorgio, *WIREs Nanomed. Nanobiotechnol.*, 2011, **3**, 620-646.

23. S. Y. Nam, L. M. Ricles, L. J. Suggs, S. Y. Emelianov, *PLoS ONE*, 2012, **7(5)**, e37267.

24. J. A. Pearce, J. R. Cook, S. Y. Emelianov, *Conf. Proc. IEEE Eng. Med. Biol. Soc.*, 2010, 2010, 2751-4.

25. Y. S. Chen, W. Frey, S. Kim, *Nano Lett.*, 2011, **11(2)**, 348-54.

26. B. Wang, S. Emelianov, *Biomedical Optics Express*, 2011, **2(11)**, 3072-3078.

27. K. Y. Lee, Y. W. Lee, K. Kwon, *Chemical Physics Letter*, 2008, **453**, 77-81.

28. P. C. Chen, S. C. Mwakwari, A. K. Oyelere, *Nanotechnology, science and applications*, 2008, **1**, 45-66.

29. D. Lapotko, *Nanomedicine (Lond)*, 2009, **4(7)**, 813-845.

30. W. Cai, T. Gao, H. Hong, *Nanotechnology, science and applications*, 2008, **1**, 17-32.

31. D. Yeager, Y.-S. Chen, S. Litovsky, S. Emelianov, *Theranostics*, 2014, **4(1)**, 36-46.

32. W. J. M. Mulder, F. A. Jaffer, Z. A. Fayad, M. Nahrendorf, *Science Translational Medicine*, 2014, **6(239)**, 239sr1 (1-11).

33. D. Jaque, L. M. Maestro, B. del Rosal, P. Haro-Gonzalez, A. Benayas, J. L. Plaza, E. M. Rodriguez, J. G. Sole, *Nanoscale*, 2014, **6**, 9494.

Description of figures

Figure 1: Design of the NANOM FIM trial.

Panel schematically represents the main design and methods of the trial. Frame (I) shows the appearance of the advanced culprit lesion before the intervention. Frame (II) depicts implantation of metal nanoparticles (NP) with bioengineered on-artery patch grown with stem cells pre-incubated in the medium with NP. Frame (III) demonstrates a detonation of NPs inside the lesion with transcatheter near-infrared (NIR) high energy laser. Frame (IV) documents a melting and shrinkage of atheroma with reduction of plaque burden and late lumen enlargement. Frame (V) shows adaptive artery remodeling with envisioned atheroregression below Glagov threshold. This technique causes late lumen enlargement, plaque reduction with integration of bioengineered on-artery scaffold to the superficial envelope of artery. Frames (VI-IX) show an alternative scenario of the NP delivery. Frame (VI) shows the phase of the NP transfer to the lesion with intravascular catheter and stem cells or microbubbles. Yellow arrows show distribution of NP in the lesion. Yellow dots designate NP. Frame (VII) demonstrates a phase of the NP detonation under NIR laser irradiation with out-body high-energy NIR device. The functionalized gold NP that form a cluster around a target molecule, and when excited with a short laser pulse, act as a heat source, thus generating an intracellular photothermal vapor bubble. Optical and mechanical effects of the bubble can be controlled through the laser parameters to tune the bubble to diagnostic or therapeutic task. Red multi-pointed stars depict a detonation of nanoparticles. A laser irradiation showed as a rose light beam. Frame (VIII) documents a melting and shrinkage of atheroma with reduction of plaque burden and late lumen enlargement. Green arrows show the shrinkage of lesion. Frame (IX) depicts adaptive artery remodeling with envisioned atheroregression below Glagov threshold. Frames (X and XI) depict stenting of the vessel with implantation (frame X) of everolimus-eluting stent with further re-endothelialization (frame XI).

Figure 2: Imaging results of the NANOM FIM trial

Panel (a) shows methodology of IVUS measurements. The cross-section for analysis is identified. External elastic membrane (EEM) and boundary of lumen are marked by red lines. Atheroma (plaque media) area is planimetered as a product of subtraction of the cross-sectional area of the lumen from the area of the EEM.

Panel (b) documents an example of atheroma regression with grey-scale and virtual histology IVUS analysis pre-, post-procedure, at 6 and 12 month follow-up in case of the micro-bubbles infusion with incorporated NP. Red lines indicate EEM and luminal boundary of the vessel wall. The atheroma area decreased from 178 to 108 mm3 with proportional changes in the lumen area.

Panel (c) depicts QCA pre-procedure and at 12 month follow up with relevant dynamics of plaque burden in IVUS frames below. A rose-marked layer of the artery wall shows boundaries of the lesion with per cent atheroma volume pre-, post-procedure and 12 month follow-up.

Panel (d) shows multi-slice CT scan frames of LAD at baseline, 6- and 12 month follow-up in patient D. treated with intracoronary infusion of micro-bubbles.

Panel (e) depicts cumulative frequency distribution curves of the mean reduction of plaque burden at 12 month follow-up in comparison with historical data of ABSORB, SATURN, ASTEROID, NANOM-PCI, PLASMONICS, and Apo-AI Milano studies. $ - analysis between Nano and Ferro groups in both populations. Panel (f) demonstrates cumulative frequency of minimal lumen diameter (intention-to-treat analysis) pre-, post- and at 12 month follow-up. * - p value for the difference between Nano group and Ferro group. ** - p value for the Nano group and stenting control. # - p value for the comparison between pre- and post-procedure values.

Figure 3: Ultrasonic results of the NANOM FIM trial in the virtual histology mode with analysis of the atheroma composition

The figure depicts changes in virtual histology tissue types. The mean percentage of dense calcium, necrotic core, fibrous and fibro-fatty tissue is reported. * - p value for the difference between Nano group and stenting control. # - p value for the Ferro group and stenting control. $ - p value for the Nano and Ferro groups. NS – non-significant (p value > 0.05).

Figure 4: Vasomotion of the coronary arteries treated with either nanotechnologies or stent

Panel (a) represents vasomotor response of coronaries to infusion of acetylcholine (Ach) and nitroglycerine (NTG). The nitroglycerine application (100 µg orally) has been following intravascular infusion of acetylcholine through a microcatheter at increasing doses up to 10-8, 10-7, 10-6 M with a washout period of at least five minutes between each dose. The figure demonstrates the more pronounced vasoactive response of the arteries in case of the nano-application.

Panel (b) shows cumulative frequency of mean lumen diameter after infusion of acetylcholine at 120, 420 and 720 seconds, and nitroglycerine – at 840 seconds. The figure underlines the higher level of the vessel wall reactivity in groups utilizing nanotechnologies if compare with stenting. Asterisk marks p value for the difference between nano-groups and stenting control.

Table 1: Baseline characteristics of the per-treatment-evaluable population (PTEP), and intention-to-treat population (ITTP).

	Nano Group		Ferro Group		Stenting Control	
	PTEP, n=42	ITTP, n=60	PTEP, n=34	ITTP, n=60	PTEP, n=40	ITTP, n=60
Age, yr	52.8±9.6	51.2±10.3	54.2±7.9	50.9±8.8	53.2±11.5	52.6±6.8
Males, no. of patients (%)	40 (95.2%)	49 (81.7%)	32 (94.1%)	44 (73.3%)	39 (97.5%)	46 (76.7%)
Body-mass index	28.4±5.5	29.2±5.2	27.6±4.8	28.1±6.1	27.5±5.4	27.8±6.2
Smoking, no. (%)						
• Never	2 (4.8%)	9 (15.0%)	2 (5.9%)	11 (18.3%)	3 (7.5%)	7 (11.7%)
• Stopped	11 (26.2%)	5 (8.3%)	15 (44.1%)	10 (16.7%)	9 (22.5%)	11 (18.3%)
• Current	29 (69.0%)	46 (76.7%)	17 (50%)	39 (65.0%)	28 (70.0%)	42 (70.0%)
Alcohol abusers, no. (%)	11 (26.2%)	29 (48.3%)	11 (32.4%)	37 (61.7%)	5 (12.5%)	25 (41.7%)
Diabetes, no. (%)	0 (0%)	0 (0%)	0 (0%)	0 (0%)	0 (0%)	0 (0%)
Hypertension needing drugs, no. (%)	40 (95.2%)	52 (86.7%)	33 (97.1%)	49 (81.7%)	39 (97.5%)	54 (90.0%)
Treated hypertension, no. (%)	39 (92.9%)	44 (73.3%)	30 (88.2%)	44 (73.3%)	38 (95.0%)	45 (75.0%)
Hyperlipidemia needing drugs, no. (%)	42 (100%)	53 (88.3%)	32 (94.1%)	51 (85.0%)	37 (92.5%)	52 (86.7%)
Treated hyperlipidemia, no. (%)	40 (95.2%)	44 (73.3%)	30 (88.2%)	42 (70.0%)	37 (92.5%)	43 (71.7%)
Previous target vessel intervention, no. (%)	0 (%)	8 (13.3%)	0 (0%)	7 (11.7%)	0 (%)	10 (16.7%)
Previous myocardial infarction, no. (%)	0 (0%)	0 (0%)	0 (0%)	0 (0%)	0 (0%)	0 (0%)
CAD, no. (%)						
• Single-vessel disease	10 (23.8%)	15 (25.0%)	8 (19.0%)	19 (31.7%)	8 (20.0%)	19 (31.7%)
• Two-vessel disease	32 (76.2%)	39 (65.0%)	26 (61.9%)	32 (53.3%)	32 (80.0%)	32 (53.3%)
• Three-vessel disease	0 (0%)	6 (10.0%)	0 (0%)	9 (15.0%)	0 (0%)	9 (15.0%)
Stable angina, no. (%)	42 (100%)	59 (98.3%)	34 (100%)	60 (100%)	40 (100%)	59 (98.3%)
• CCS Class I	6 (14.3%)	21 (35.0%)	1 (2.9%)	24 (40.0%)	8 (20.0%)	22 (36.7%)
• CCS Class II	36 (85.7%)	38 (63.3%)	33 (97.1%)	36 (60.0%)	32 (80.0%)	37 (61.7%)
• CCS Class III	0 (0%)	0 (0%)	0 (0%)	0 (%)	0 (0%)	0 (0%)
Unstable angina, no. (%)	0 (0%)	0 (0%)	0 (0%)	0 (0%)	0 (0%)	0 (0%)
Silent ischemia, no. (%)	0 (0%)	1 (1.7%)	0 (0%)	0 (0%)	0 (0%)	1 (1.7%)
NYHA functional class of heart failure, no. (%)						
• Class I	0 (%)	0 (0%)	0 (%)	0 (0%)	0 (%)	0 (0%)
• Class II	27 (64.3%)	38 (63.3%)	22 (64.7%)	43 (71.7%)	28 (70.0%)	41 (68.3%)
• Class III	15 (35.7%)	22 (36.7%)	12 (35.3%)	17 (28.3%)	12 (30.0%)	19 (31.7%)
• Class IV	0 (%)	0 (0%)	0 (%)	0 (0%)	0 (%)	0 (0%)
ASS, no. (%)	42 (100%)	60 (100%)	34 (100%)	60 (100%)	40 (100%)	60 (100%)
Clopidogrel, no. (%)	41 (97.6%)	49 (81.7%)	34 (100%)	52 (86.7%)	39 (97.5%)	59 (98.3%)
Target vessel, no. (%)						
• Left anterior descending	31 (73.8%)	35 (58.3%)	21 (61.8%)	32 (53.3%)	33 (82.5%)	29 (48.3%)
• Left circumflex	6 (14.3%)	14 (23.3%)	9 (26.5%)	10 (16.7%)	5 (12.5%)	13 (21.7%)
• Right coronary artery	5 (11.9%)	11 (18.3%)	4 (11.8%)	18 (30.0%)	2 (5.0%)	18 (30.0%)
AHA/ ACC lesion classification, no. (%)						
• A	0 (0%)	3 (5.0%)	0 (0%)	4 (6.7%)	0 (0%)	4 (6.7%)
• B1	19 (45.2%)	29 (48.3%)	19 (55.9%)	34 (56.7%)	25 (62.5%)	31 (51.7%)
• B2	23 (54.8%)	26 (43.3%)	15 (44.1%)	21 (35.0%)	15 (37.5%)	23 (38.3%)
• C	0 (%)	2 (3.3%)	0 (%)	1 (1.7%)	0 (0%)	2 (3.3%)
Pre-procedure SYNTAX score, <22 only	16.5±8.2	18.5±5.2	15.8±6.1	16.5±6.5	15.8±5.4	15.9±8.2
Mean diameter of reference vessel, mm	2.62±0.64	2.68±0.51	2.61±0.37	2.61±0.69	2.73±0.85	2.74±0.45
Minimal lumen diameter (MLD), mm	1.11±0.32	1.12±0.38	1.06±0.29	1.08±0.44	1.06±0.28	1.06±0.24
Maximal lumen diameter, mm	1.58±0.69	1.62±0.92	1.43±0.78	1.55±0.82	1.64±0.65	1.62±0.47
Mean lumen diameter, mm	1.32±0.74	1.35±0.81	1.28±0.66	1.29±0.78	1.39±0.71	1.40±0.69
Diameter stenosis, %	67.2±15.3	68.1±14.3	69.5±12.7	65.3±19.6	70.2±12.4	71.4±18.4
Lesion length, mm	8.22±2.16	8.12±4.68	8.94±4.82	9.03±5.26	8.74±4.04	8.85±3.92
Plaque burden (percent atheroma volume, PAV), %	69.3±16.5	68.5±12.3	69.9±14.6	69.4±12.2	70.8±15.2	68.4±14.4
Total plaque-media volume (total atheroma volume – TAV), mm^3	179.2±81.3	178.4±85.7	182.6±78.5	183.1±96.1	184.2±62.8	175.8±94.4
Lumen volume, mm^3	79.4±33.5	82.1±34.5	78.5±42.5	80.6±39.9	75.8±36.5	81.4±42.7
VH-IVUS:						
• Dense calcium, %	7.19±5.43	7.54±5.11	8.35±6.14	8.75±6.13	8.76±8.72	8.89±9.02
• Necrotic core, %	18.65±7.26	18.85±8.13	17.83±9.13	17.94±8.14	18.20±8.58	18.22±9.25
• Fibrous tissue, %	58.65±14.22	58.09±15.36	58.47±14.26	58.21±16.92	59.33±16.85	59.11±18.92
• Fibro-fatty, %	15.51±7.23	15.52±8.46	15.35±6.61	15.09±7.37	13.71±8.47	13.78±9.56
VH-IVUS:						
• Dense calcium, mm^2	0.32±0.30	0.34±0.32	0.37±0.32	0.40±0.36	0.39±0.39	0.40±0.36
• Necrotic core, mm^2	0.83±0.69	0.85±0.64	0.79±0.66	0.82±0.79	0.81±0.64	0.82±0.79
• Fibrous tissue, mm^2	2.61±1.22	2.62±1.38	2.59±1.34	2.66±1.42	2.64±1.37	2.66±1.42
• Fibro-fatty, mm^2	0.69±0.48	0.70±0.49	0.68±0.43	0.69±0.48	0.61±0.55	0.62±0.46

Data are mean (SD) or number (%). CCS = Canadian Cardiovascular Society classification of angina pectoris. AHA/ACC = American Heart Association/ American College of Cardiology. Difference

between groups and subsets is non-significant. Continuous variables are expressed as mean±SD (standard deviation).

Table 2: Angiographic and IVUS findings post-procedure and at 12-month imaging follow-up

	Nano Group		Ferro Group		Stenting Control		ANOVA, *p value*	
Number of enrolled patients, no.	60		60		60		NA	
Imaging and clinical follow-up (intention-to-treat population, ITTP), no. (%)	60 (100%)		60 (100%)		60 (100%)		NA	
Imaging and clinical follow-up (per-treatment-evaluable population, PTEP), no (%)	42 (70.0%)		34 (56.7%)		40 (66.7%)		NA	
Imaging post-procedure (PTEP/ ITTP populations)								
Minimal lumen diameter (MLD), mm	1.16±0.54	1.19±0.42	1.29±0.44	1.37±0.69	2.26±0.84	2.42±0.62	< 0.01	< 0.01
Maximal lumen diameter, mm	1.64±0.32	1.69±0.74	1.59±0.94	1.75±1.01	3.01±0.99	3.03±0.84	0.031	0.042
Mean lumen diameter, mm	1.39±0.63	1.44±0.72	1.35±0.73	1.42±0.82	2.41±1.15	2.44±1.09	> 0.05 < 0.01[#]	> 0.05 < 0.01[#]
Per cent stenosis, %	53.2±14.8	54.8±19.3	46.1±18.4	41.6±24.9	7.5±2.9	10.3±8.4	< 0.01	< 0.01
Plaque burden (percent atheroma volume, PAV), %	60.0±18.4	59.9±17.2	59.9±15.3	60.3±16.8	54.4±26.6	54.6±29.3	> 0.05 0.031[#]	> 0.05 0.032[#]
Total plaque-media volume (total atheroma volume – TAV), mm^3	142.3±62.7	144.5±59.9	147.9±62.2	148.9±82.2	178.4±51.9	179.1±63.3	0.031	0.029
Lumen volume, mm^3	95.2±55.9	96.5±61.3	98.8±48.4	97.9±53.9	149.4±49.1	148.9±45.5	> 0.05 < 0.01[#]	> 0.05 < 0.01[#]
VH-IVUS:								
• Dense calcium, %	8.14±4.12	8.13±3.58	8.72±3.12	8.95±2.28	9.19±6.68	9.50±8.54	0.012	0.019
• Necrotic core, %	50.68±14.13	50.77±12.96	42.66±11.63	42.51±9.63	34.98±9.84	34.99±11.37	< 0.01	< 0.01
• Fibrous, %	30.54±9.26	30.33±11.42	35.78±9.92	35.57±8.14	48.88±9.67	48.38±10.42	0.022	0.027
• Fibro-fatty, %	10.63±3.78	10.77±2.79	12.84±3.14	12.98±2.96	6.95±4.02	7.13±4.16	0.039	0.035
VH-IVUS:								
• Calcium, mm^2	0.36±0.31	0.37±0.33	0.38±0.24	0.40±0.53	0.41±0.48	0.44±0.42	> 0.05	0.049
• Necrotic core, mm^2	2.24±0.48	2.31±0.84	1.86±0.72	1.90±0.65	1.56±0.52	1.62±0.63	0.038	0.035
• Fibrous, mm^2	1.35±0.63	1.38±0.56	1.56±0.62	1.59±0.74	2.18±1.02	2.24±1.06	0.026	0.042
• Fibro-fatty, mm^2	0.47±0.22	0.49±0.26	0.56±0.29	0.58±0.36	0.31±0.12	0.33±0.17	0.041	0.018
Imaging at 12-month follow-up (PTEP/ ITTP populations)								
SYNTAX score	19.6±9.6	19.8±6.4	18.4±6.1	17.9±8.2	17.4±6.1	17.7±6.7	< 0.01	0.024
Minimal lumen diameter (MLD), mm	3.11±0.47	3.08±0.52	3.00±0.84	2.98±0.63	2.87±0.62	2.82±0.32	< 0.01	< 0.01
Maximal lumen diameter, mm	4.26±1.15	4.33±1.03	3.92±0.74	3.96±0.83	3.09±0.75	3.16±0.92	< 0.01	< 0.01
Mean lumen diameter, mm							> 0.05	> 0.05
• Baseline	4.02±0.66	4.03±0.69	3.72±0.86	3.76±0.68	2.89±0.63	2.91±0.47	0.018[#]	0.021[#]
• Ach	4.15±0.32	4.15±0.34	3.81±0.41	3.91±0.55	2.84±0.72	2.88±0.69	0.029[#]	< 0.01[#]
• NTG	4.29±0.34	4.21±0.42	3.92±0.23	3.99±0.39	2.91±0.45	2.95±0.46	< 0.01[#]	< 0.01[#]
Lesion length, mm	7.21±3.52	7.43±5.11	7.72±5.12	8.03±6.13	7.98±5.22	7.85±6.38	< 0.01	0.031
Binary restenosis rate							> 0.05	> 0.05
• On-site of intervention	1 (2.38%)	2 (3.33%)	2 (5.88%)	2 (3.33%)	5 (12.5%)	6 (10.0%)	0.041[#]	0.041[#]
• In-segment	1 (2.38%)	2 (3.33%)	2 (5.88%)	2 (3.33%)	5 (12.5%)	6 (10.0%)	> 0.05 0.041[#]	> 0.05 0.041[#]
Plaque burden (percent atheroma volume, PAV), %	38.4±12.6	37.8±13.9	40.7±11.8	39.4±12.8	52.4±16.6	52.9±15.8	> 0.05 0.021#	> 0.05 0.024#
Total plaque-media volume (total atheroma volume – TAV), mm^3	107.5±41.5	108.2±42.2	117.9±73.7	115.6±64.0	176.1±45.5	178.0±52.6	0.033	0.029
Lumen volume, mm^3	172.3±92.2	178.3±99.4	171.8±72.8	177.7±86.3	159.9±82.5	158.4±78.7	> 0.05 < 0.01[#]	> 0.05 < 0.01[#]
VH-IVUS:								
• Dense calcium, %	6.39±2.14	6.57±1.92	6.45±2.02	6.01±1.85	2.66±1.82	2.83±1.69	0.042	0.022
• Necrotic core, %	28.19±10.51	28.47±9.53	26.45±8.36	26.58±9.36	24.69±9.93	25.47±10.05	> 0.05	> 0.05
• Fibrous, %	49.25±11.63	48.91±12.96	51.29±11.95	50.95±12.04	61.50±9.75	60.38±9.92	0.048	0.039
• Fibro-fatty, %	16.17±9.15	16.06±8.53	15.81±9.28	16.46±8.15	11.14±3.64	11.32±3.84	0.043	> 0.05
VH-IVUS:								
• Calcium, mm^2	0.17±0.09	0.18±0.07	0.20±0.14	0.19±0.17	0.11±0.09	0.12±0.11	0.044	0.049
• Necrotic core, mm^2	0.75±0.32	0.78±0.51	0.82±0.56	0.84±0.39	1.02±0.52	1.08±0.36	0.048	0.046
• Fibrous, mm^2	1.31±0.49	1.34±0.91	1.59±0.36	1.61±0.42	2.54±1.24	2.56±1.64	< 0.01	< 0.01
• Fibro-fatty, mm^2	0.43±0.16	0.44±0.39	0.49±0.14	0.52±0.32	0.46±0.38	0.48±0.25	> 0.05	0.051

* - *p-value* for the difference between Nano and Ferro groups;
[#] - *p-value* for the difference between Nano and Control groups;
NA – non-available, or not applicable. Continuous variables are expressed as mean±SD.
Table 3: Clinical follow-up (one event per patient) at 12 months after the intervention (intention-to-treat analysis)

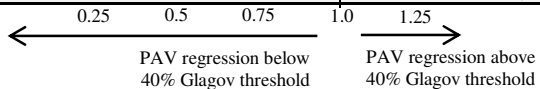|	Nano Group	Ferro Group	Stenting Control	ANOVA, *p value*
Number of enrolled patients, no.	60	60	60	NA
Event-free survival (all cause), no. (%)	55 (91.7%)	49 (81.7%)	48 (80.0%)	0.031* 0.068
Target lesion cardiac death, no. (%)	0 (0%)	0 (0%)	1 (1.7%)	> 0.05
Target vessel cardiac death, no (%)	0 (0%)	2 (3.3%)	1 (1.7%)	0.091
Non-cardiac death, no. (%):	5 (8.3%)	9 (15.0%)	10 (16.7%)	0.032*, 0.064
• Stroke	2 (3.3%)	3 (5.0%)	5 (8.3%)	> 0.05
• Trauma	2 (3.3%)	4 (6.7%)	4 (6.7%)	> 0.05
• Cancer	1 (1.7%)	1 (1.7%)	1 (1.7%)	>0.05
• Others	0 (0%)	1 (1.7%)	0 (0%)	>0.05
Target lesion myocardial infarction, no. (%)	0 (0%)	0 (0%)	2 (3.3%)	> 0.05
Target vessel myocardial infarction, no. (%)	3 (5.0%)	6 (10.0%)	4 (6.7%)	0.029*, 0.059
Target lesion revascularization (TLR), no. (%)	2 (3.3%)	2 (3.3%)	4 (6.7%)	0.058, 0.039[#]
Target vessel revascularization (TVR), no. (%)	6 (10.0%)	12 (20.0%)	8 (13.3%)	0.061, 0.043[#]
Thrombosis of culprit artery, no. (%)	0 (0%)	1 (1.7%)	4 (6.7%)	0.074, 0.028[#]
• ARC definite thrombosis	0 (0%)	1 (1.7%)	4 (6.7%)	0.074, 0.028#
Newcomers with diabetes mellitus, no. (%)	9 (15.0%)	8 (13.3%)	5 (8.3%)	0.058
• Insulin-dependent	2 (3.3%)	1 (1.7%)	3 (5.0%)	> 0.05
Newcomers with SYNTAX score ≥23, no. (%)	4 (6.7%)	8 (10.0%)	7 (11.7%)	0.042*, 0.071

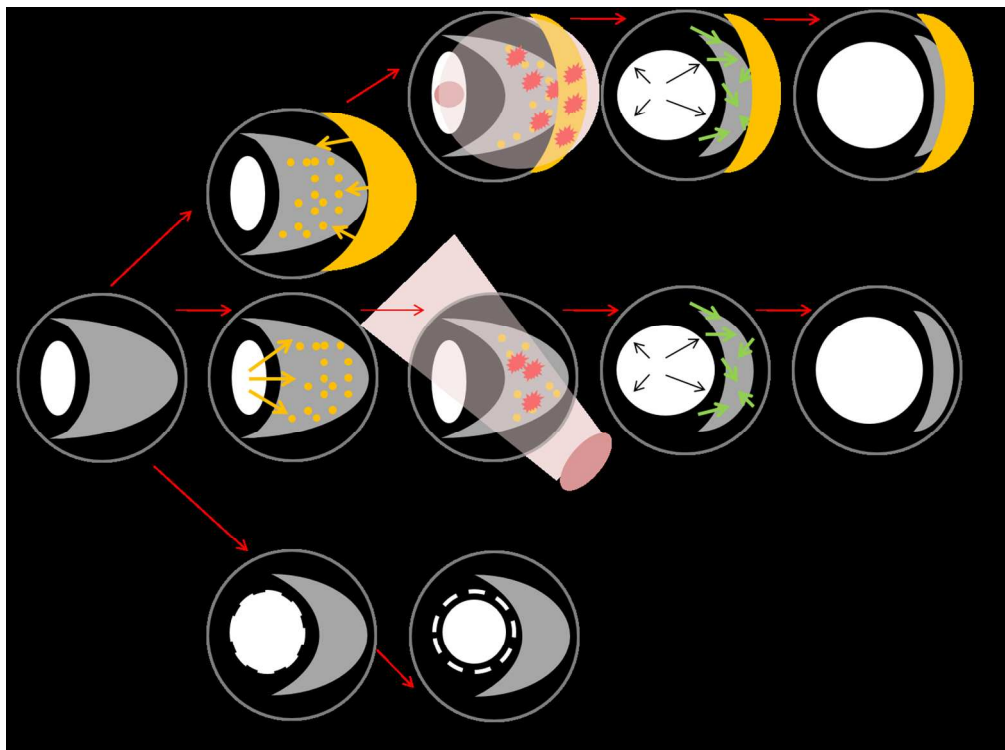* - p-value for the difference between Nano and Ferro groups;

\# - p-value for the difference between Nano and Control groups;

NA – non-available, or not applicable. Continuous variables are expressed as mean ± SD. ARC – Academic Research Consortium. The definition of definite on-site thrombosis was tailored to the type of intervention.
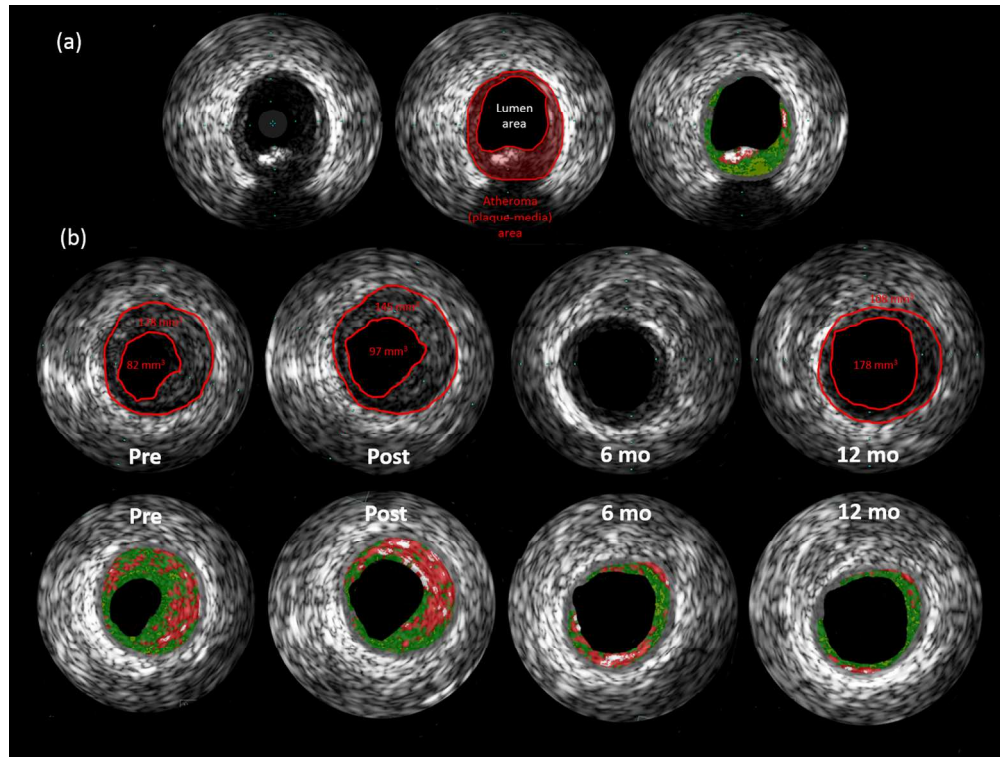
Table 4: Prespecified subgroup analysis of change in plaque burden from baseline to follow-up at 12 months (intention-to-treat analysis)

Characteristic	No.	Hazard ratio (95% CI)		*p value* for intervention (ANOVA)	*p value* for interaction
Sex, no. of patients					0.80
Male				0.96	
Nano	49		0.92 (0.73 to 1.06)		
Ferro	44		0.89 (0.69 to 1.09)		
Stent	46		0.92 (0.76 to 1.07)		
Female				0.79	
Nano	11		0.78 (0.49 to 0.99)		
Ferro	16		0.85 (0.56 to 1.05)		
Stent	14		0.89 (0.63 to 1.06)		
Smoking, no.					0.27
Never				0.09	
Nano	9		0.75 (0.64 to 0.94)		
Ferro	11		0.57 (0.43 to 0.98)		
Stent	7		0.62 (0.59 to 0.88)		
Stopped/ Current				0.89	
Nano	51		0.89 (0.76 to 1.19)		
Ferro	49		0.81 (0.68 to 1.14)		
Stent	53		0.87 (0.72 to 1.19)		
Alcohol abuse, no.					0.97
Yes				0.94	
Nano	29		0.57 (0.36 to 1.01)		
Ferro	37		0.69 (0.45 to 0.87)		
Stent	25		0.64 (0.33 to 0.94)		
No				0.98	
Nano	31		0.93 (0.59 to 1.12)		
Ferro	23		0.87 (0.85 to 1.11)		
Stent	35		0.85 (0.69 to 1.06)		
Baseline PAV, %					0.79
< Mean				0.97	
Nano	22		0.89 (0.66 to 1.01)		
Ferro	21		0.85 (0.58 to 0.98)		
Stent	26		0.86 (0.55 to 0.93)		
≥ Mean				0.78	
Nano	38		0.43 (0.16 to 0.49)		
Ferro	39		0.32 (0.01 to 0.62)		
Stent	34		0.38 (0.09 to 0.72)		
Baseline MLD, mm					0.84
< Mean				0.72	
Nano	36		0.32 (0.16 to 0.73)		
Ferro	33		0.39 (0.04 to 0.58)		
Stent	31		0.49 (0.34 to 0.69)		
≥ Mean				0.92	
Nano	24		0.69 (0.49 to 0.87)		
Ferro	27		0.75 (0.58 to 0.77)		
Stent	29		0.77 (0.54 to 0.94)		
Baseline calcium, mm²*					0.97
< Mean				0.99	
Nano	28		0.74 (0.54 to 0.85)		
Ferro	23		0.69 (0.58 to 0.88)		
Stent	25		0.76 (0.54 to 0.86)		
≥ Mean				0.96	
Nano	32		0.49 (0.37 to 0.61)		
Ferro	37		0.53 (0.39 to 0.66)		
Stent	35		0.64 (0.54 to 0.68)		
Baseline necrotic core, mm²*					0.047
< Mean				0.031	
Nano	36		0.46 (0.39 to 0.49)		
Ferro	39		0.58 (0.52 to 0.71)		
Stent	33		0.74 (0.64 to 0.85)		
≥ Mean				0.048	
Nano	24		0.73 (0.56 to 0.98)		
Ferro	21		0.87 (0.76 to 0.97)		
Stent	27		0.39 (0.34 to 0.72)		
Baseline fibrous, mm²*					0.63
< Mean				0.41	
Nano	28		0.56 (0.36 to 0.86)		
Ferro	23		0.37 (0.14 to 0.53)		
Stent	24		0.54 (0.34 to 0.78)		
≥ Mean				0.69	
Nano	32		0.55 (0.35 to 0.80)		
Ferro	37		0.48 (0.28 to 0.70)		
Stent	36		0.56 (0.37 to 0.63)		
Baseline fibro-fatty, mm²*					0.068
< Mean				0.83	
Nano	29		0.75 (0.55 to 1.01)		
Ferro	26		0.78 (0.50 to 0.99)		
Stent	24		0.79 (0.53 to 0.93)		
≥ Mean				0.049	
Nano	31		0.75 (0.61 to 1.06)		
Ferro	34		0.54 (0.35 to 0.68)		
Stent	36		0.69 (0.55 to 1.01)		

0.25   0.5   0.75   1.0   1.25

← PAV regression below 40% Glagov threshold
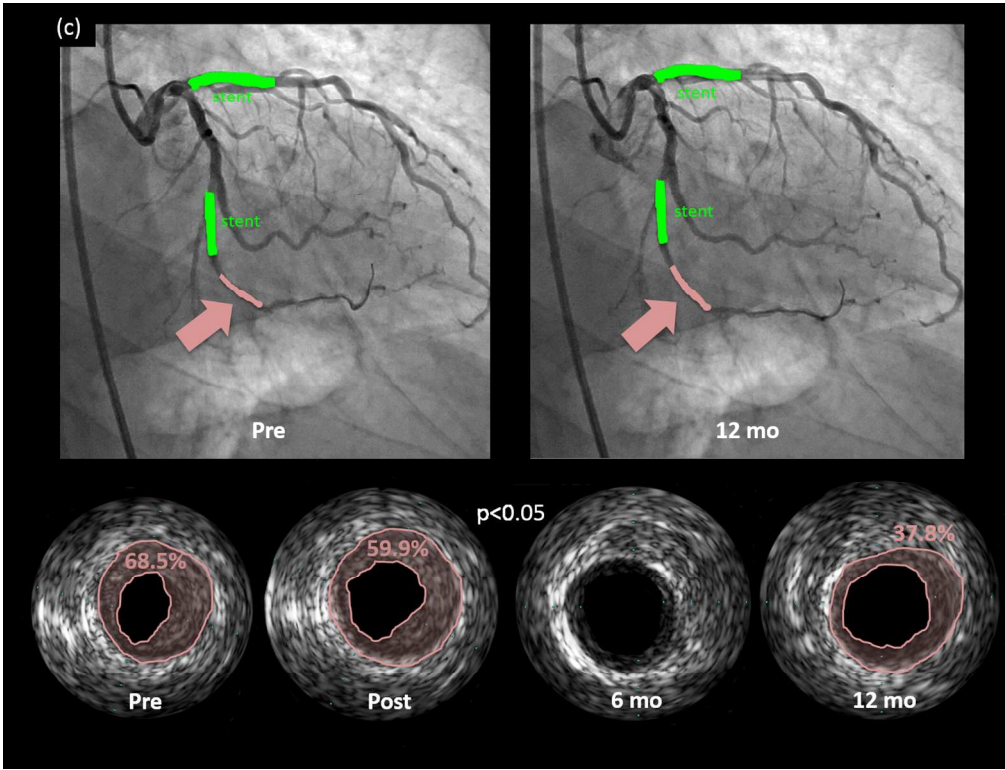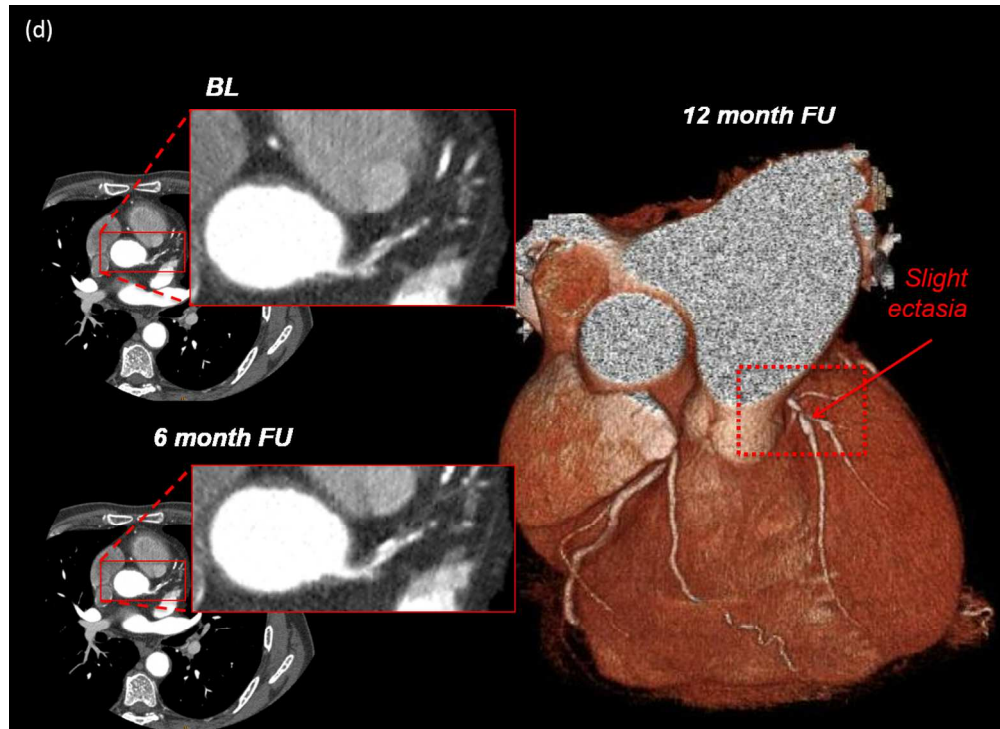
→ PAV regression above 40% Glagov threshold

248x184mm (150 x 150 DPI)

263x197mm (150 x 150 DPI)

257x197mm (150 x 150 DPI)

(d)

BL

12 month FU

Slight ectasia

6 month FU
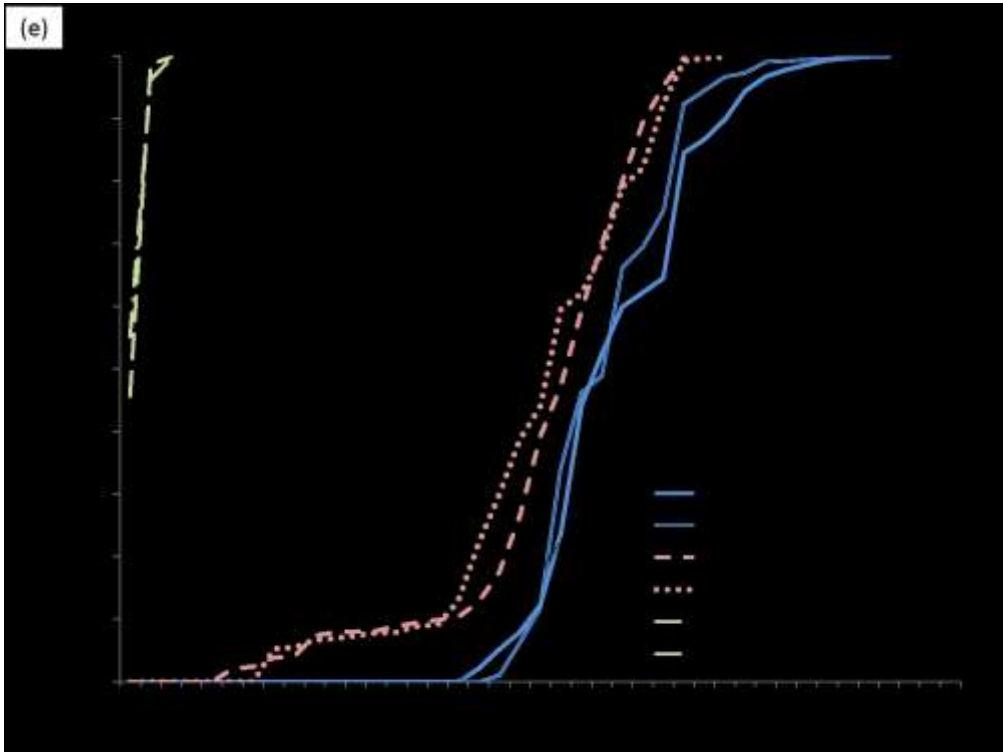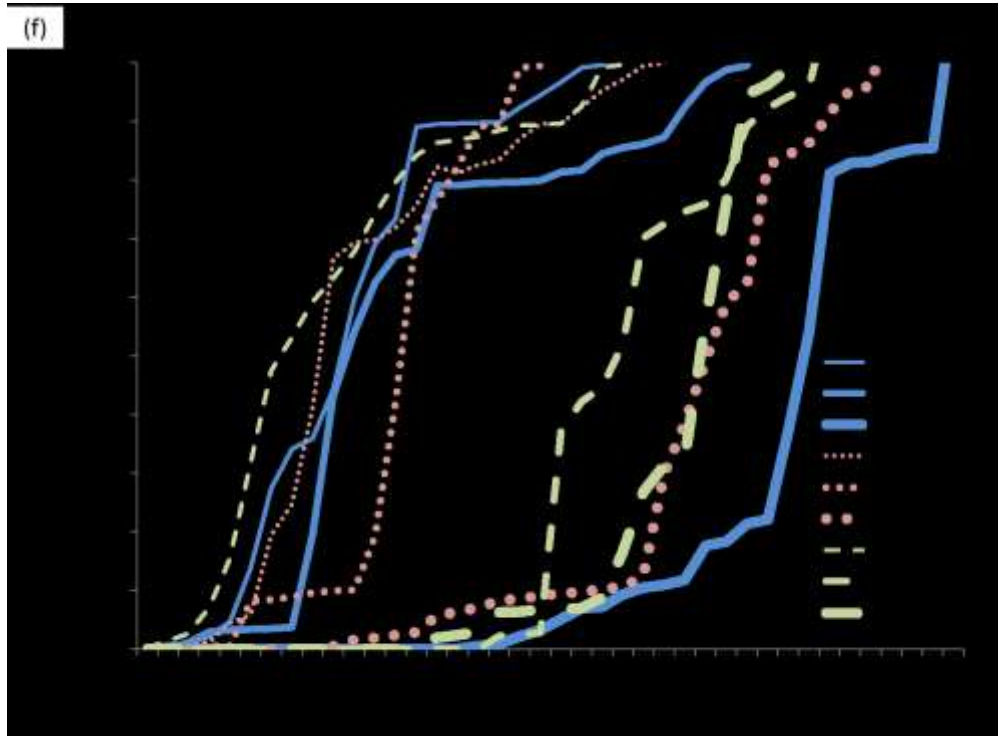
252x183mm (150 x 150 DPI)

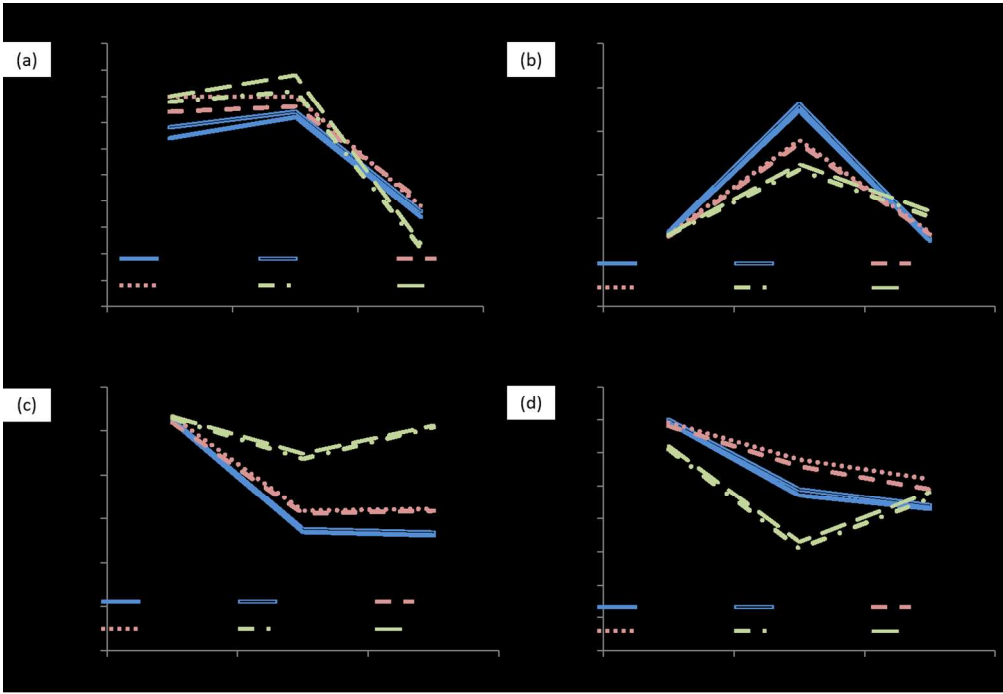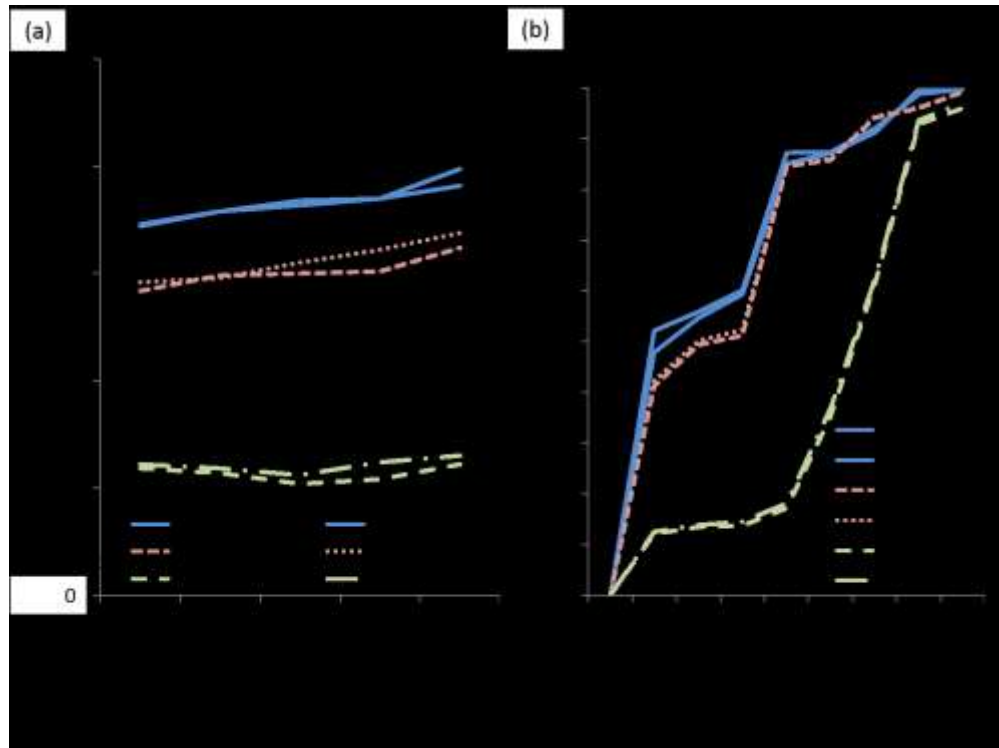246x184mm (150 x 150 DPI)

246x180mm (150 x 150 DPI)

250x172mm (150 x 150 DPI)

251x187mm (150 x 150 DPI)